Supporting Information for "Comparing gravity waves in a high resolution run of the IFS to AIRS satellite observations and ERA5"

Emily J. Lear[1], Corwin J. Wright[1], Neil P. Hindley[1], Inna Polichtchouk[2],

Lars Hoffmann [3]

[1]Centre for Climate Adaptation and Environment Research, University of Bath, Bath, UK

[2]European Centre for Medium-Range Weather Forecasts, Reading, UK

[3]Jülich Supercomputing Center, Forschungszentrum Jülich, Jülich, Germany

Contents of this file

1. AIRS noise granules (Figures S1 – S3)

2. 8 µm Brightness temperatures for the AIRS swaths shown in the example case studies in Figures 3–6 (Figure S4)

3. U and v components of the wind speed for the example case studies in Figures 3–6 (Figure S5)

4. Mean horizontal wavelengths (Figure S6)

5. Horizontal wavelengths for each night in the first 10 days of November 2018 (Figure S7)

6. Statistics for the bivariate histograms in Figure 9 (Table S1)

7. Point-wise correlations between IFS 1 and 2 (Table S2)

―――――

September 28, 2023, 10:41am

Introduction

This document includes figures and tables to support the methods and results. Figures include the AIRS noise granules used to add noise to the resampled model data (Figures S1–S3) and Figures S4 and S5, which show the brightness temperature and winds for the example case studies in Figures 3–6 of the paper. The mean horizontal wavelength in the region and time period investigated and the horizontal wavelengths for each night are shown in Figures S6 and S7, respectively. Tables S1 and S2, show statistics for the data used for the bivariate histograms (Figure 9 of the paper).

AIRS noise granules (Figures S1 – S3)

Figures S1 – S3 show the temperature perturbations of the AIRS granules, at 39 km altitude, containing only nighttime data with no subjectively clear visible waves that were used to add noise to the resampled model data. Each granule was also flipped in along-track and across-track directions to obtain 30 noise granules in total for each region (polar, mid latitudes and tropics).

AIRS 8 μm Brightness temperatures for the example case studies in Figures 3–6 (Figure S4)

Figure S4 shows the 8 μm brightness temperatures for the AIRS swaths shown in the example case studies (Figures 3 – 6). The temperature perturbations of the AIRS swaths are shown in Figure 3a and 5a for the AIRS swath in Figure S4a and b, respectively. Regions where the brightness temperature is below 220 K are classified as deep convection (outlined in pink in the figure).

U and v components of the wind speed for the example case studies in Figures 3–6 (Figure S5)

September 28, 2023, 10:41am

The u and v components of the wind speed are shown in Figure S5 for the example case studies on the 5th and 9th November 2018 in Figures 3–6 of the paper.

Mean horizontal wavelengths (Figure S6)

The mean horizontal wavelengths for nighttime data in the first 10 days of November 2018 are shown for AIRS and the resampled models in Figure S6. Areas of noise are reduced by finding where the amplitude smoothed by a 7 x 7 point boxcar is below the 70th percentile for each data set and removing data points in these locations.

The mean horizontal wavelengths in each data set are generally similar in areas of peak gravity wave activity. There is a feature at the centre of the y axis on the left with longer horizontal wavelengths in AIRS (Figure S6a) that can not be clearly seen in the other data sets. This long horizontal wavelength wave is only seen on the 5th night of the first 10 nights of November 2018 (see Supplementary Figure S7), but most of the noise is removed from that area for the other nights and is not included in the mean, so the wavelengths appear much longer than for most of the rest of the region.

Horizontal wavelengths for each night in the first 10 days of November 2018 (Figure S7)

In Figure S7, the horizontal wavelength data used to calculate the the mean horizontal wavelengths in Figure S6 are shown for each night (1–10) in the the first 10 days of November 2018. Areas of noise were reduced by removing data points where the amplitude, smoothed with a 7 by 7 point boxcar filter, is below the 70th percentile for each data set.
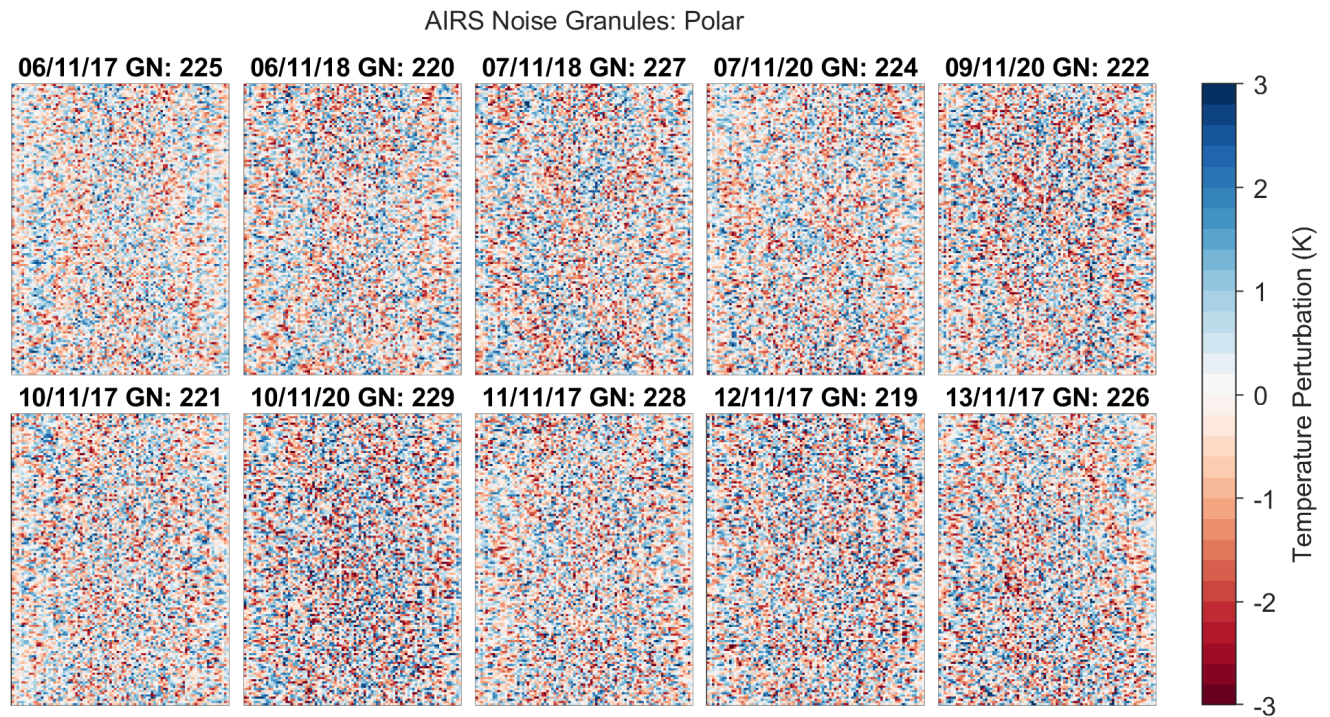
Statistics for the 2D histograms (Table S1)

September 28, 2023, 10:41am

Table S1 shows the point numbers included in the panels in Figure 9 and fractions of points above and below the grey dashed 1:1 lines for each panel.
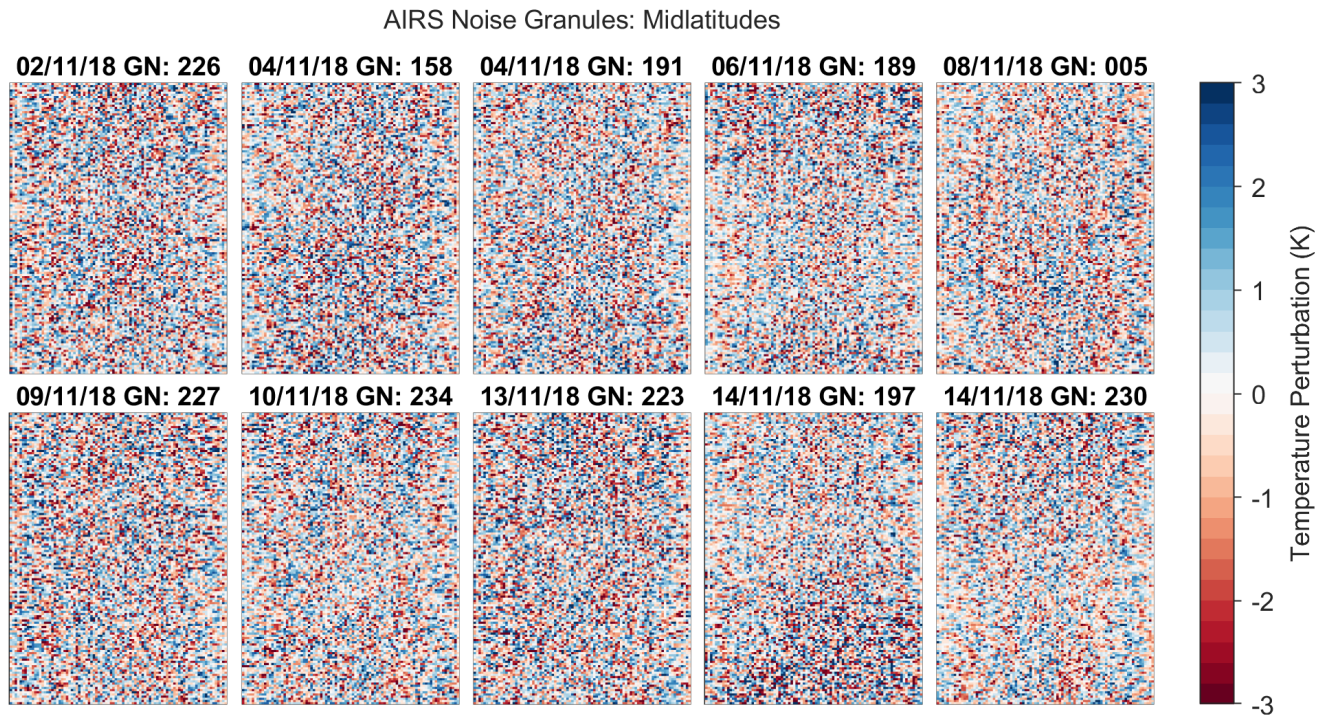
Point-wise correlations between IFS 1 and 2 (Table S2)

The point-wise correlation coefficients between the IFS run resampled using method 1 (IFS 1) and 2 (IFS 2) are shown in Table S2 with AIRS noise added (noise) and before adding noise (no noise). The correlation coefficients with AIRS noise added are calculated using the same data used for the bivariate histograms in Figure 9a–d, with areas of noise reduced by removing data points where the amplitude, smoothed with a 7 by 7 point boxcar filter, is below the 70th percentile for each data set.
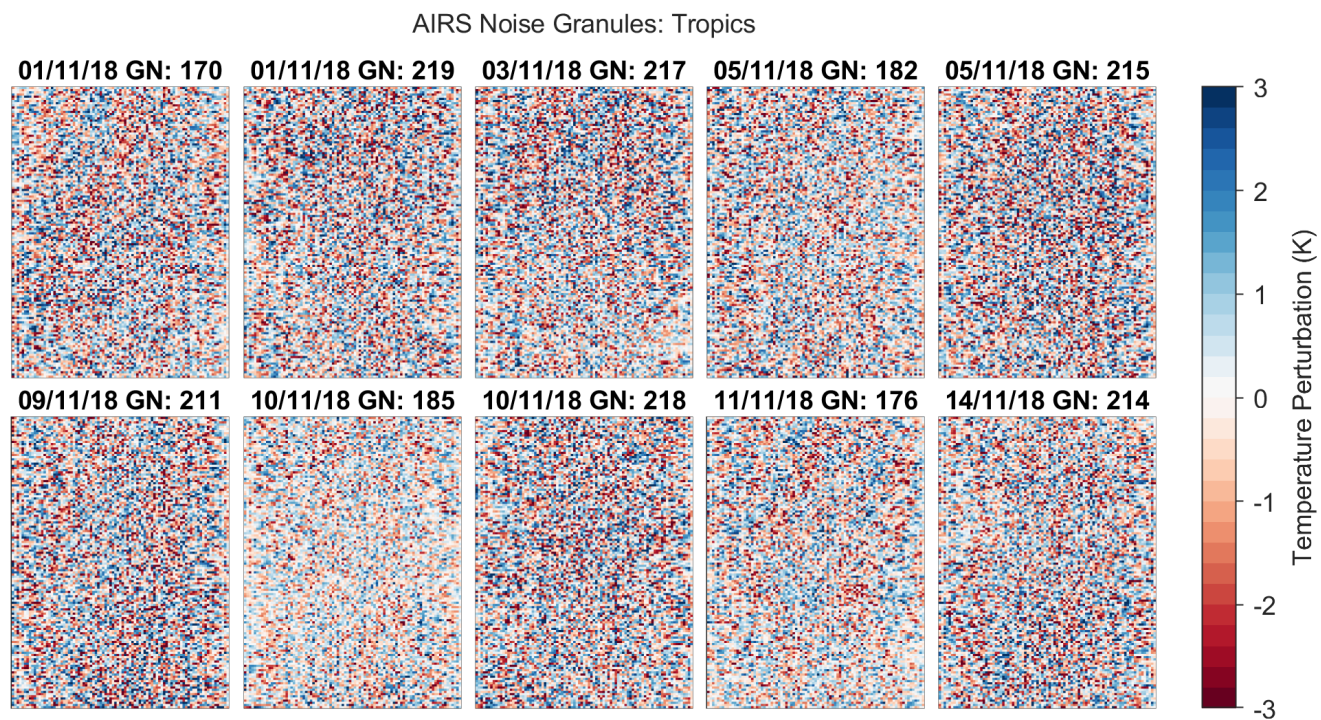
These correlations are all positive and, with AIRS noise added, are highest for the horizontal wavelength (0.511) and lowest for the momentum flux (0.227). Some of the difference between these results for the 1 km IFS run resampled using both methods will be due to the added AIRS noise, as the AIRS noise granules added to the data were chosen randomly for both data sets. Without AIRS noise added the correlation is highest for the amplitude (0.762) and lowest for the vertical wavelength (0.378). The horizontal wavelength correlation coefficient is lower without AIRS noise added (0.453), compared to after adding noise (0.511), but only the areas where the amplitude was over the 70th percentile for IFS 1 and 2 were included for the data with AIRS noise added which will affect these results.
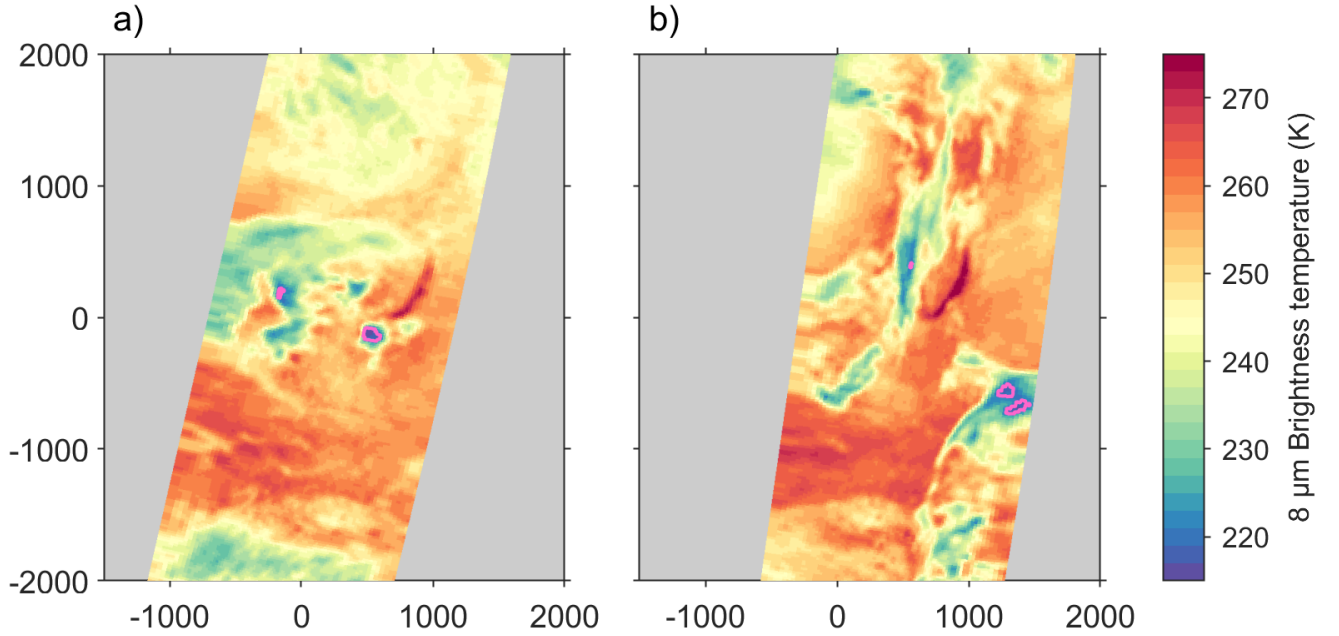
AIRS Noise Granules: Polar

Figure S1. AIRS temperature perturbations at 39 km altitude for granules with no clear visible gravity waves, and over 10 % of the data in the region investigated (Figure 1) containing mostly polar data (>60° latitude). The data has a horizontal point spacing of ~20 km in the across track direction (x-axis) and ~18 km in the along track direction (y-axis). The measurement date is shown above each granule and the granule number (GN).
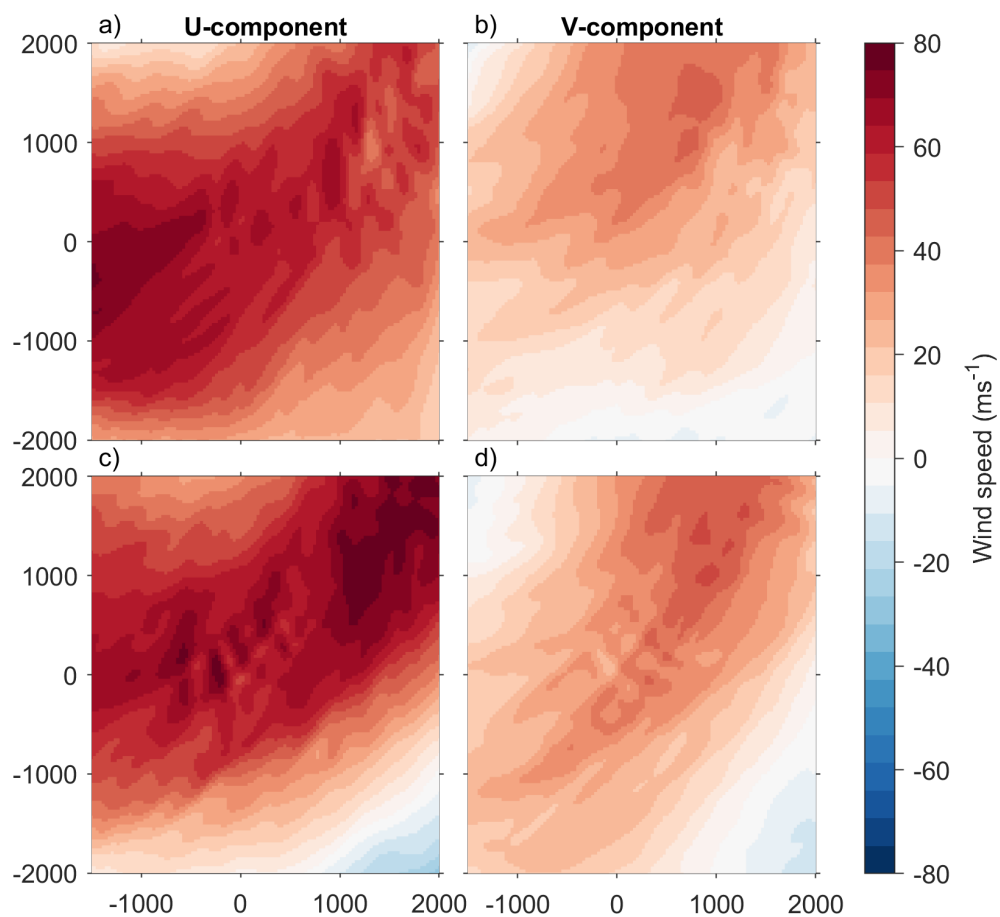
Figure S2. As in Figure S1, but for AIRS granules containing mostly data in the mid latitudes (>30° and <60° latitude).

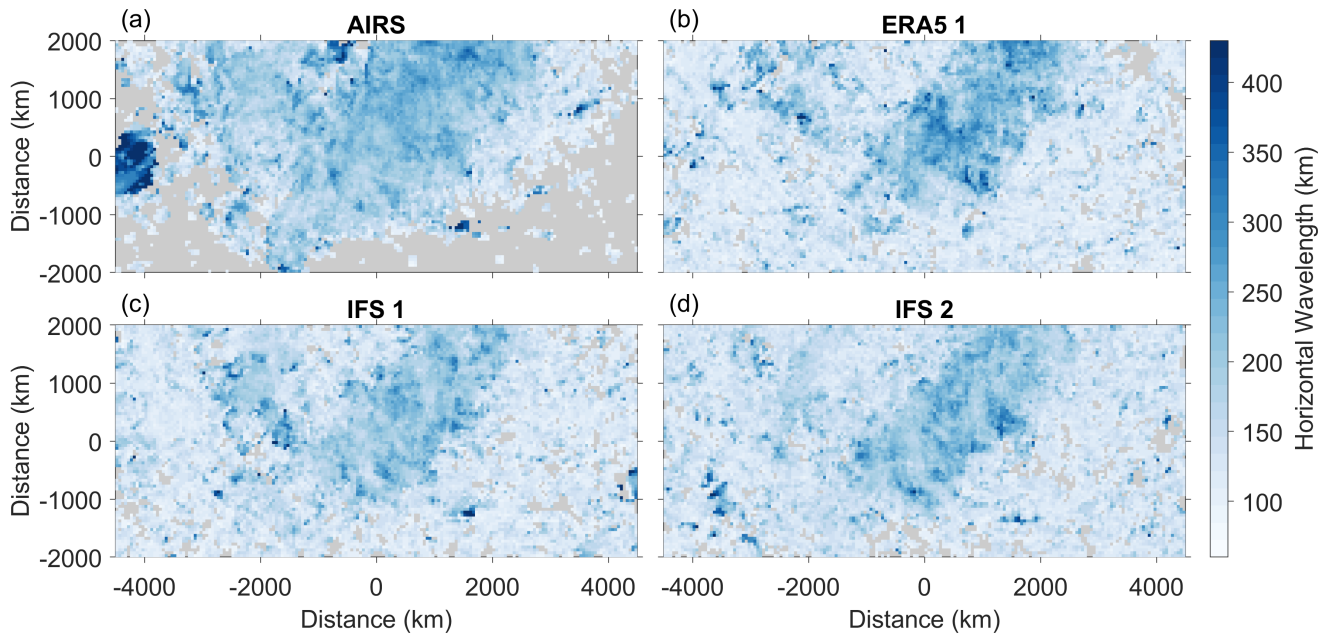**Figure S3.** As in Figure S1, but for AIRS granules containing mostly data in the tropics (<30°
latitude).

Figure S4. 8 µm Brightness Temperatures for AIRS swaths at 39 km altitude interpolated to a regular distance grid with a horizontal spacing of 5 km and centre (0,0) at 52° latitude, 94° longitude. a) on the 5th November with average granule times from 19:38 - 19:50 UTC and b) on the 9th November with average granule times from 19:14 and 19:26 UTC. Areas where the brightness temperature is below 220 K (classified as deep convection (Hoffmann & Alexander, 2010)) are outlined in pink.

Figure S5. U (a and c) and v (b and d) components of the wind speed at 39 km altitude for the example case studies on the 5th November (a and b) and on the 9th November (c and d) in 2018.

Figure S6. Mean horizontal wavelength in the region shown in Figure 1 at 39 km altitude for nighttime data in the first 10 days of November 2018. Data points where the amplitude, smoothed by a 7×7 point boxcar filter, is below the 70th percentile for each data set are removed.

September 28, 2023, 10:41am

Figure S7. Horizontal wavelengths in the region shown in Figure 1 at 39 km altitude for AIRS and the resampled models, for each night in first 10 nights of November 2018. Areas where the amplitude, smoothed by a 7×7 point boxcar filter, is below the 70th percentile in each data set are removed.

September 28, 2023, 10:41am

		IFS 1 & IFS 2	AIRS & IFS 1	AIRS & IFS 2	AIRS & ERA5 1	IFS 1 & ERA5 1	IFS 2 & ERA5 1
	num	83564	95018	94863	92646	72051	68483
A	f_a	0.496	0.177	0.185	0.141	0.453	0.453
	f_b	0.504	0.823	0.815	0.859	0.547	0.547
HW	f_a	0.557	0.436	0.469	0.472	0.504	0.456
	f_b	0.443	0.564	0.531	0.528	0.444	0.544
VW	f_a	0.531	0.336	0.332	0.443	0.567	0.565
	f_b	0.469	0.664	0.668	0.557	0.433	0.435
MF	f_a	0.483	0.212	0.212	0.192	0.455	0.477
	f_b	0.517	0.788	0.788	0.808	0.545	0.523

Table S1. Table showing number of points included in the bivariate histograms in Figure 9 (num), fraction of points above (f_a) and below (f_b) the 1:1 lines (grey dashed lines in Figure 9) for the amplitude (A), horizontal (HW) and vertical (VW) wavelengths and the momentum flux (MF). Points on the 1:1 lines are not included in the fractions.

	Amplitude	Horizontal Wavelength	Vertical Wavelength	$\log_{10}$(Momentum Flux)
noise	0.379	0.511	0.350	0.227
no noise	0.761	0.453	0.378	0.715

Table S2. Point-wise correlation coefficients for the wave properties between the 1 km IFS resampled as AIRS using both methods (IFS 1 and 2) in nighttime for the first 10 days of November 2018. The correlation coefficents are shown with AIRS noise added (noise) and before AIRS noise was added (no noise). Noise is reduced in the data with AIRS noise added using the same method as for Figures 8 and 9.